Lawrence Berkeley Laboratory
UNIVERSITY OF CALIFORNIA

ENERGY & ENVIRONMENT
DIVISION

To be presented at the American Society of Mechanical Engineers, Solar Energy Division, Conference on Systems Simulation, Economic Analysis/Solar Heating and Cooling Operational Results, Reno, NV, April 27-May 1, 1981

INTERACTION OF A SOLAR SPACE HEATING SYSTEM WITH THE THERMAL BEHAVIOR OF A BUILDING

Christian Vilmer, Mashuri L. Warren, and
David Auslander

December 1980

Prepared for the U.S. Department of Energy under Contract W-7405-ENG-48

DISCLAIMER

INTERACTION OF A SOLAR SPACE HEATING SYSTEM WITH THE THERMAL BEHAVIOR OF A BUILDING*

Christian Vilmer+, Mashuri L. Warren

Solar Energy Group
Lawrence Berkeley Laboratory

David Auslander

Dept. of Mechanical Engineering
University of California, Berkeley

ABSTRACT

The thermal behavior of a building in response to heat input from an active solar space heating system is analysed to determine the effect of the variable storage tank temperature on the the cycling rate, on-time, and off-time of a heating cycle and on the comfort characteristics of room air temperature swing and of offset of the average air temperature from the setpoint (droop).

A simple model of a residential building, a fan coil heat-delivery system, and a bimetal thermostat are used to describe the system. A computer simulation of the system behavior has been developed and verified by comparisons with predictions from previous studies. The system model and simulation are then applied to determine the building response to a typical hydronic solar heating system for different solar storage temperatures, outdoor temperatures, and fan coil sizes. The simulations were run only for those cases where there was sufficient energy from storage to meet the building load requirements.

For given conditions of outdoor temperature, anticipation, and thermostat setpoints, the storage tank temperature has a direct effect on droop and swing. The higher the storage tank temperature, the larger is the swing in room temperature, and the smaller is the offset of the average air temperature from the setpoint (droop). The results indicate that to maintain room temperatures within comfort limits by minimizing both swing and droop, a hydronic solar space heating system requires a control system that adjusts anticipation and setpoints in relation to the outdoor and the storage tank temperatures. This will require more than a simple on-off bimetal thermostat.

NOMENCLATURE

t	Time variable.
s	Laplace transform variable.
T_{air}	room air temperature
T_{win}	Temperature of the interior wall.
T_{wex}	Temperature of the interior surface of the exterior wall.
T_{out}	Outdoor temperature.
τ_1	Shortest building time constant.
τ_2	Intermediate building time constant.
τ_3	Longest building time constant.
τ_{BM}	Thermostat bimetal strip time constant.
α	Ratio of influence of interior wall and room air temperatures on thermostat.
T_{fict}	Effective temperature seen by thermostat because of room and interior wall.
R_{fict}	Effective thermal resistance from thermostat to room and interior wall.
P_{ant}	Anticipator heating power.
ΔT_{ant}	Anticipator gain. $\Delta T_{ant} = P_{ant} R_{fict}$
ϵ	Fan coil heat exchanger effectiveness.
C_{min}	Fan coil thermal capacitance flow rate. $C_{min} = \dot{M}_A C_A$, where $\dot{M}_A$ is the air mass flow rate and C_A is the thermal heat capacity of air.
F_{fan}	Fan coil sizing ratio. $\epsilon C_{min}/UA_B$

*This work has been supported by the Systems Analysis and DesignBranch, SystemsDevelopment Division, Office of Solar Applications, U.S. DOE, under Contract No. W-7405-ENG-48.
+Present address, 38 Rue General Delestraint, 75016, Paris, France.

τ_p Fan coil delivery time constant.

P(t) Heat input power from a fan coil or a furnace ductwork, which transfers energy directly to the air within the space.

UA_B Effective building loss constant.

INTRODUCTION

The thermal behavior of a building in response to heat input from an active solar space heating system is analysed to determine the effect of a variable storage tank temperature on the comfort characteristics droop and swing during a heating cycle. This work was undertaken to understand and evaluate the control characteristics required for the residential heating load simulator of the experimental solar controls test facility at Lawrence Berkeley Laboratory [1]. The interaction of baseboard, radiant panel, and furnace heating systems with thermostat control of building temperature has been extensively studied [2,3,4,5,6,7,8]. However, the effects on building comfort of an active solar heating system where the power delivered changes with storage tank temperature has not been previously examined in detail.

The study is divided into four parts: 1) modeling of the building, heat-delivery system, and thermostat; 2) computer simulation of the system; 3) sensitivity analysis applied to a conventional fan coil heating system sized at 130 % of design load to verify performance of the model; and 4) application of the system model and simulation to determine the building response to the solar heating system.

SYSTEM MODEL

The system model includes the house, the thermostat, and the heat-delivery system. The building is modeled as a three node capacitance-resistance network. The thermostat temperature is modeled as a single node network related only to the interior wall and air temperatures and anticipator power input. The anticipator is a small electrical heater that is energized (in a heating thermostat) only when the switch is on. The function of the anticipator is to minimize the overshoot of the room air temperature and thereby reduce the temperature swing. The heat delivery system is modeled as a fan-coil heat exchanger. The fan coil output power into the room depends on the storage tank temperature, airflow rates, and fan coil heat exchanger effectiveness.

The performance of a heat delivery, thermostat, and building system is simulated as follows: At each time step the temperatures of the room air (T_{air}), the inside wall (T_{win}), the exterior wall (T_{wex}), and the thermostat (T_{BM}) are computed and the thermostat temperature is compared with the thermostat setpoints to determine the system operating condition. To accurately determine the cycle time, the time step can be as short as 3 seconds. Because the outdoor temperature changes only slowly over several hours and to simplify the analysis, the outdoor temperature, T_{out}, is kept constant during the simulation. The initial conditions for the wall temperatures were chosen close to the steady state temperatures. The simulations are run for sufficient time to insure that a steady state condition is reached where the temperature of the walls and room air repeat during each cycle. The values of the duty cycle, average and extreme room air temperatures, and final wall temperatures are then saved on an output file.

Two types of heating systems have been used for the simulations. A typical hot water fan coil with a constant hot water inlet temperature and sized to give 130% of the design heating load was used to verify the model and to examine the sensitivity of the model to different system parameters. Then a heating system with a fan-coil heat exchanger sized for a solar system was modeled to examine the effect of different storage tank temperatures on system performance.

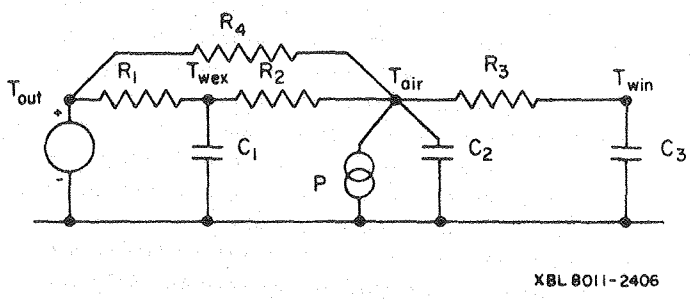

Figure 1. The dynamic building model uses three resistance capacitance nodes to represent the temperatures of the interior and exterior walls, T_{win} and T_{wex}, and the room air, T_{air}. The heat input to the air, P, is represented as a thermal current source.

The Building Model.

A three node capacitance-resistance network model of a single zone residence was used to study the dynamic response of a building to heat input. Simplified network models are often used to evaluate thermostat and heat-delivery system performance [7,8,9]. The heat input is provided directly to the air, for example, as when a heating fan coil is turned on. The three nodes shown in Figures 1 and 2 represent the temperatures of the interior surface of the exterior wall, $T_{wex}(t)$, the temperature of the air in the space, $T_{air}(t)$, and the temperature of the interior wall, $T_{win}(t)$ The equations for the temperatures are determined from the resistance-capacitance network, using Kirchhoff analysis. The values of the thermal resistances R_1, R_2, R_3, and R_4, and the ther-

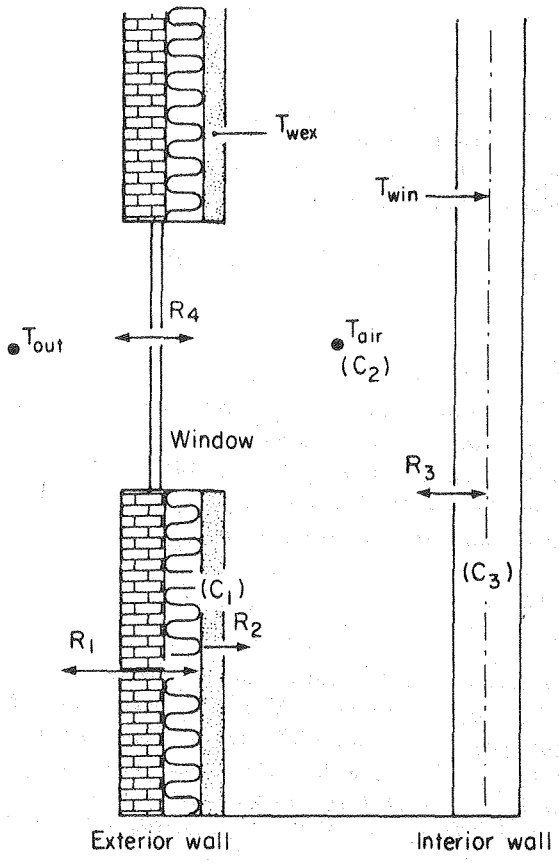

XBL8011-2408

Figure 2. Single zone building model showing representative thermal resistances and capacitances.

mal capacitances C_1, C_2, and C_3 are typical of a well insulated single zone building. The input power to heat the space, P, is represented as a thermal current source. This three node room model has been discussed previously [10].

Laplace transform analysis is used to determine the time-constants of the building system, τ_1, τ_2, and τ_3. The resulting expressions for $T_{wex}(s)$, $T_{air}(s)$, $T_{win}(s)$ are a function of the Laplace Transform of the input power, P(s) .

Thermostat Model.

The heating system of a building is controlled by the thermostat. The thermostat is composed of three parts: a bimetallic temperature sensor, a snap-action switch, and an anticipator. The bimetal strip responds to the temperature by bending more or less and causing the switch to make or break. The "snap-action" switch is a two-position control element with a "switch-differential", that gives different on- and off- temperatures. The switch differential is typically less than 0.6°C (1 °F). Since the bimetal strip does not react instantaneously to changes in air temperature, the air temperature can rise far above the desired temperature when the furnace is on. The additional heat provided by the anticipator increases the bimetal temperature causing the switch to turn off sooner.

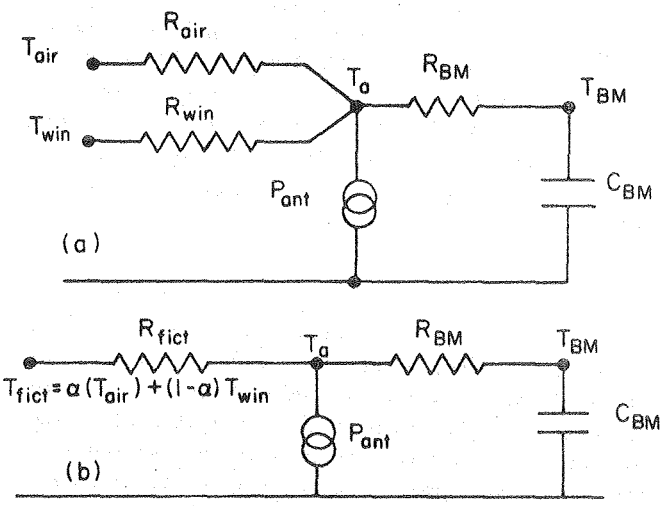

XBL8011-2407

Figure 3. The thermostat can be represented as a thermal network.

(a) The bimetal temperature, T_{BM}, is affected by the interior wall and room air temperatures.

(b) Equivalent network model of thermostat.

The thermostat bimetal element responds to both the temperatures of the room air, T_{air}, and of the interior wall to which it is attached, T_{win}. This is adequately described by a single time-constant model [9,11,12] with a time-constant, τ_{BM}, of about 5 to 8 minutes. As only a single time-constant is used to represent the thermostat bimetallic strip, only one thermal capacitance is needed in the thermostat model. Figure 3 shows a model of the thermostat and the corresponding thermal resistance network. The response of the thermostat to room air and wall temperatures can be approximated by a fictitious temperature T_{fict}:

$$T_{fict} = \alpha T_{air} + (1-\alpha) T_{win} .$$

The effective heat transfer resistance, R_{fict}, can be shown to be simply related to R_{win}, R_{air}, and α.

The equation for the temperature of the bimetal, $T_{BM}(t)$, including the effect of the anticipator can be derived from thermal network shown in Figure 3b. The corresponding Laplace transform $T_{BM}(s)$ is given by;

$$T_{BM}(s) = \frac{T_{fict}(s)}{(1 + s\tau_{BM})} + \frac{\Delta T_{ant}}{s(1 + s\tau_{BM})} + \frac{\tau_{BM} T_{BM}(0)}{(1 + s\tau_{BM})}$$

As $T_{fict}(s)$ is a linear combination of $T_{air}(s)$ and $T_{win}(s)$, T_{BM} will depend on the initial temperatures of the walls and is affected by building dynamics. The bimetal temperature as a function of time can be solved from the expressions for the wall and outdoor temperatures. The anticipator gain, $\Delta T_{ant} = P_{ant} R_{fict}$, is proportional to the power of the anticipator.

Fan coil model.

The performance of a hydronic heating system is modeled to determine the effects of thermostat control on occupant comfort. Hot water goes to a fan-coil heat exchanger to heat the air delivered to the room. For a conventional system with heat source is a boiler with an output temperature of 180°F. For a solar system, the heat source is solar heated water at the storage tank temperature.

The steady state power, P_o, delivered by a fan coil depends on the air inlet and outlet temperatures and air flow capacitance rate, C_{min}.

$$P_o = C_{min} [T_{airout} - T_{airin}]$$

Using a simple model for a cross flow heat exchanger, the power delivered from the heat exchanger can also be shown to depend on the difference between the air and water inlet temperatures, the capacitance rate, and the heat exchanger effectiveness, ϵ.

$$P_o = \epsilon C_{min} [T_{waterin} - T_{airin}]$$

To simplify the calculation, we assume that the fan coil water inlet temperature, $T_{waterin}$ is at the storage temperature, T_{stor}, and is constant during the simulation period. The inlet air temperature, T_{inair}, is equal to the room air temperature, T_{air}. Therefore, the steady state fan coil power is given by

$$P_o = \epsilon C_{min} [T_{stor} - T_{air}].$$

Because of delays due to thermal losses in the duct work heat is delivered into the room with a power P(t) which is represented as a single time constant system [3,13,14].

$$P(t) = Po\ (1 - e^{-t/\tau_P})$$

where the Laplace transform is given by

$$P(s) = \frac{Po}{(1 + s\tau_P)}$$

For a fan coil delivery heating system the time constant is typically about 1 minute. It takes a certain time for air outlet temperature, T_{airout}, to reach an equilibrium temperature.

$$T_{airout}\ (t) = T_{inair} + (P_o/C_{min})\ (1-e^{-t/\tau_P})$$

Fan coil sizing.

For an active solar heat delivery system to be effective, the fan coil must be properly sized to meet the anticipated building load. The design load depends on the effective building heat loss constant, UA_B, and the design temperature, T_{Design}.

$$P_{Design} = UA_B(T_{room} - T_{Design})$$

For example, with a winter design temperature of $T_{Design} = -23°C$ (-10 °F), and a heat loss constant, $UA_B = 264$ W/°C (500 Btu/hr-°F), and a room temperature of $T_{room} = 20°C$ (68 °F), the design heating load is about $P_{Design} = 11.4$ kW (40 kBtu/hr). The recommended fan coil sizing [17] for an active solar system is

$$F_{fan} = \frac{\epsilon C_{min}}{UA_B} = 2.$$

For $F_{fan} = 2$ and a fan coil heat exchanger effectiveness, $\epsilon = 0.7$, this requires a capacitance rate of $C_{min} = 754$ W/°C (1430 Btu/hr-°F), or an air volume flow of 37 m^3/min (1300 ft^3/min). At a storage temperature of about 82°C (180 °F), this gives a fan coil output power of 32 kW (110 kBtu/hr), or about three times the design building load.

SYSTEM SIMULATION

The Laplace transform equations giving the building and thermostat temperatures are solved using Cramer's rule. The inverse Laplace transforms are taken to determine the temperatures as a function of time. The resulting equations are then used in a computer program simulating the behavior of the heating system, the response of the building, and the control action of the thermostat for different outside temperatures. The program computes the temperatures of the house and of the thermostat at each step of the simulation. At the end of each time step, the ther-

mostat bimetal temperature is compared to the on and off thermostat set points and the control of the heat delivery system is set for the next time step. The behavior of the heating system is described using the characteristics shown in Table 1. At the end of each cycle, the cycle characteristics are computed. Once steady state is reached, the characteristics of the last cycle are written out to a data file.

On-time:	time during which the furnace stays on.
Off-time:	time during which the furnace stays off.
Cycle time:	length of a cycle; on-time plus off-time.
Duty cycle:	percentage of on-time in the cycle. This is determined by the ratio of coil capacity to load.
Cycle rate:	number of on-off cycles per hour.
Swing:	difference between the maximum and minimum room air temperatures reached during the cycle.
Droop:	difference between the desired temperature (the lower thermostat setpoint) and the average room temperature during the cycle.

Table 1. Performance characteristics of the heating cycle.

Verification of Sensitivity Analysis.

To verify the simulation program, several sensitivity studies of a conventional hydronic heating system were done to examine carefully the influence of system time constants and other parameters on the steady state behavior of the heating system. These parameters have have been given reasonable values either chosen from the literature [11,12,3,14], or justified by the sensitivity analysis. The values for cycling rate, temperature swing and droop as functions of duty cycle showed a general agreement with those published in the literature [2,15,11,12,3,14]. This verification gives us confidence that our model adequately describes the interaction between the room, heat delivery system, and thermostat.

Building parameters. The thermal capacitances and resistances of the building corresponded to an empty house with a single zone. The thermal capacitance of the room air, C_2, has been doubled to take into account the thermal mass of the furnishings. This assumption is commonly made in the literature [3]. This leads to the doubling of the short time-constant of the house, τ_1. The temperature response of the room air is therefore slower, and the swing will be reduced by a factor of 2, to more reasonable values.

The time constants for the building model are determined from the thermal capacitances and resistances of the model. The longest time-constant τ_3 describes the relaxation of the temperature of the total building thermal mass to the outside temperature. The short time-constant τ_1 is directly related to the heat transfer from the room air to the walls and to the outside. The intermediate time-constant τ_2 is related to the redistribution of energy within the space. Typical system parameters for a well insulated building used in the simulation are listed in Table 2.

Thermostat parameters. The important thermostat parameters are: α, a coefficient specifing the relative importance of interior wall and air temperatures; τ_{BM}, the bimetal time-constant; the switch-differential; and the anticipator power, P_{ant}. Other parameters, such as thermal resistance of the thermostat box, can be identified from detailed thermal modeling, however their effects are already described by these four major parameters.

The coefficient α determines the relative impact of the wall and air temperatures on the the bimetal temperature. α has only a slight influence on the behavior of the system. Swing, cycling rate, and on-time change very little, as α varies from .25 to 1.0. An increase of α leads to a slight decrease of the cycle rate, and a slight increase of swing. α has no effect on droop and duty cycle. Since the choice is not crucial, $\alpha = 0.5$ has been used for the simulations. The influence of α has also been discussed by K.M. Letherman [9].

Thermal Resistances

$1/R_1$ = 128 W/°C (243. Btu/hr-°F)
$1/R_2$ = 1640 W/°C (3111. Btu/hr-°F)
$1/R_3$ = 344 W/°C (653. Btu/hr-°F)
$1/R_4$ = 147 W/°C (279. Btu/hr-°F)
$1/R_{eff}$ = 266 W/°C (504. Btu/hr-°F)

Thermal Capacitances

C_1 = 4.69 MJ/°C (2470. Btu/°F)
C_2 = 0.93 MJ/°C (490. Btu/°F)
C_3 = 1.97 MJ/°C (1036. Btu/°F)

Time constants.

τ_1 = 0.107 hrs
τ_2 = 1.301 hrs
τ_3 = 8.153 hrs

Table 2. Typical parameters for a typical well-insulated residence treated as a single zone [15]. R-21 walls, R-32 ceiling, and R-17 floor. Floor area 158 m^2 (1700 ft^2). Glazing 19 m^2 (200 ft^2). Infiltration 2/3 air change per hour.

The bimetal time-constant has a direct influence on swing, but almost no effect on duty cycle, cycling rate and droop. A decrease of the bimetal time-constant leads to a decrease of swing. A bimetal time constant τ_{BM} = 6.8 minutes has been chosen from McBride [11,12].

The switch differential has a direct effect on swing and on-time, but no effect on the duty-cycle. This leads to an effect on cycling rate. The switch differential has a small influence on droop. Reducing the switch differential leads to a decrease of on-time and swing and to an increase in droop and cycle rate. Typical thermostat constants chosen from the literature and used as a base case for the simulations are shown in Table 3.

Effect of anticipation. Simulations have been run with the above parameters, for different outside temperatures. The results are shown in Figure 4, 5, and 6. The cycle rate, droop, and swing at 50 % duty cycle are shown in Table 4. The values for heating system characteristics such as cycle rate, droop, and swing, are in accordance with values found by others [2,15,11,16,6].

Parameter	Value
Bimetal time-constant:	T_{BM} = 6.8 min
Switch Differential:	0.44 °C (0.79 °F)
Coefficient c:	0.50
Furnace Time-constant:	τ_p = 1.0 min.
Furnace Power:	P_o = 130% Designed Heat Load
Anticipator gain:	ΔT_{ant} = 0.3 to 1.7 °C (0.5 to 3.0 °F)

Table 3. Parameters used in the simulations

ΔT_{ant} °F	Cycle Rate Cycles/hr	Droop °F	Swing °F
0.5	3.2	+0.2	5.3
1.0	3.8	-0.1	4.6
2.0	5.6	-0.6	3.1
3.0	8.0	-1.1	2.0

Table 4. Effect of anticipation on cycle rate, droop, and swing for a conventional heat system at 50% duty cycle. Design heat load 16 kW (32 kBtu/hr). Heat delivery P_o = 21.8 kW (41.4 kBtu/hr). $T_{waterin}$ = 180°F. C_{min} = 538 Btu/hr-°F.

The anticipator has a dominant affect on swing and droop: as the anticipation is increased, droop increases and the swing decreases. An increase in anticipation leads to an increase of cycling rate, and to a decrease of the on-time. For a given outdoor temperature, the duty cycle is almost constant and depends on the ratio of load to fan coil capacity.

As shown in Figure 4, the shape of the curve of cycling rate versus duty cycle is almost symmetrical with a maximum cycling rate for a duty cycle of 50%. This is commonly reported in the literature. For most outside temperatures with an anticipation gain, ΔT_{ant}, of less than 2 °F, the cycling rate is less than 5 cycles per hour also in agreement with others [2,11,12,3,4,14].

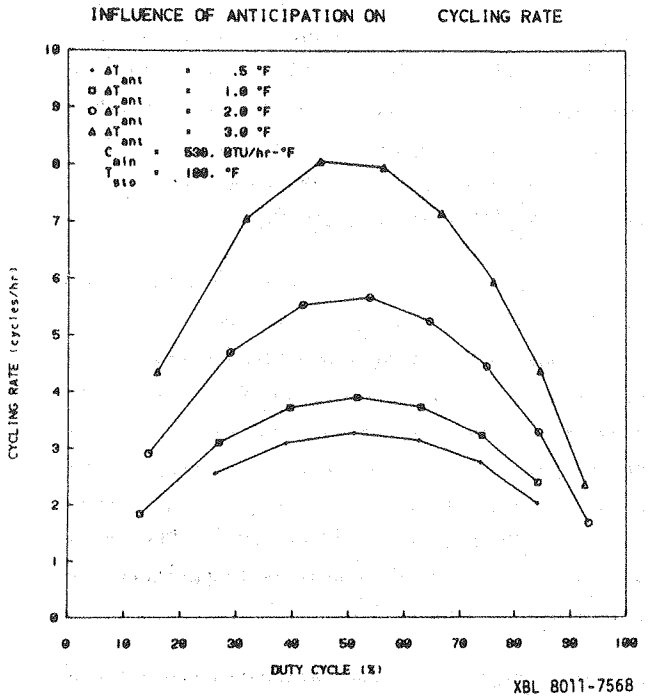

Figure 4. The cycling rate is a maximum at a 50 % duty cycle. The symmetrical shape of the curve is typical. As the anticipation is increased, the cycling rate increases.

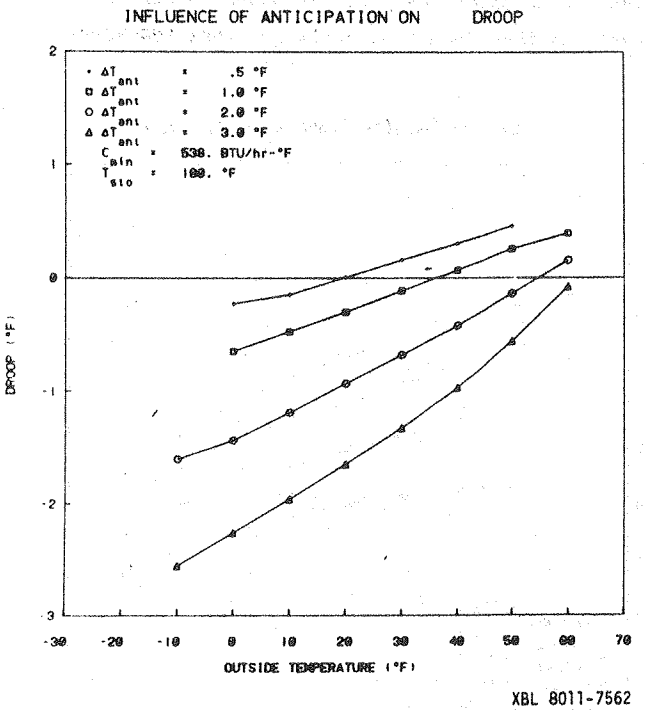

Figure 5. Droop is dominated by the anticipation. Droop increases as the anticipation is increased and as the outside temperature becomes colder.

Figure 5 shows that droop is an almost linear function of the duty cycle going from $0^{o}F$ to about $3^{o}F$ for an anticipator gain of 3 ^{o}F. Anticipation is the only control parameter that strongly effects droop. The affects of the other parameters on droop appear to be negligible. This is in agreement with results from literature[2,11,12]. With larger anticipation the thermostat on time is shorter producing less heating on a single cycle. The average room air and interior wall temperatures drop, so that the thermostat bimetal cools off faster, reducing the off-time. After several cycles, approximately the same duty cycle is restored to meet the load. However, the cycle rate is higher and there is an an offset (known as droop) of the average room air temperature from the set temperature. Because the heating system is on and off for shorter times, the room air temperature swings are also reduced.

Room temperature swing is the most sensitive characteristic of a cycle. The major influences on swing are the bimetal time-constant, the anticipation, and the thermostat switch differential. The bimetal time-constant introduces a delay in the response of the thermostat, and therefore allows overshoots and undershoots of the air temperature. The anticipation reduces swing by turning off the thermostat sooner and thereby reducing the overshoot.

The swing as a function of duty cycle for different anticipation gains are shown in Figure 6. At 50% duty cycle swing can be reduced from 5.3 ^{o}F for a small anticipation (ΔT_{ant} = 0.5 ^{o}F) to 2 ^{o}F for a large anticipation (ΔT_{ant} = 3.0 ^{o}F). This reduction of swing is less for duty cycles greater than 80 %, which correspond to low outside temperatures. The switch differential represents the lower limit of swing and its influence is less important than anticipation and the bimetal time-constant.

Solar heating system simulations.

Thermostat performance as measured by droop, swing, and duty cycle has been calculated for an active solar heating system with different storage tank temperatures ranging from 49 ^{o}C ($120^{o}F$) to 82 ^{o}C ($180^{o}F$). This has the effect of increasing the effective heat-delivery system power from 26 to 58 kW (50 to 110 kBtu/hr). The storage tank temperature was held constant for each simulation.

We used an outside design temperature of $-10^{o}F$ (corresponding to Madison, WI) and a room temperature of $70^{o}F$. Using the design criteria given by Beckman,

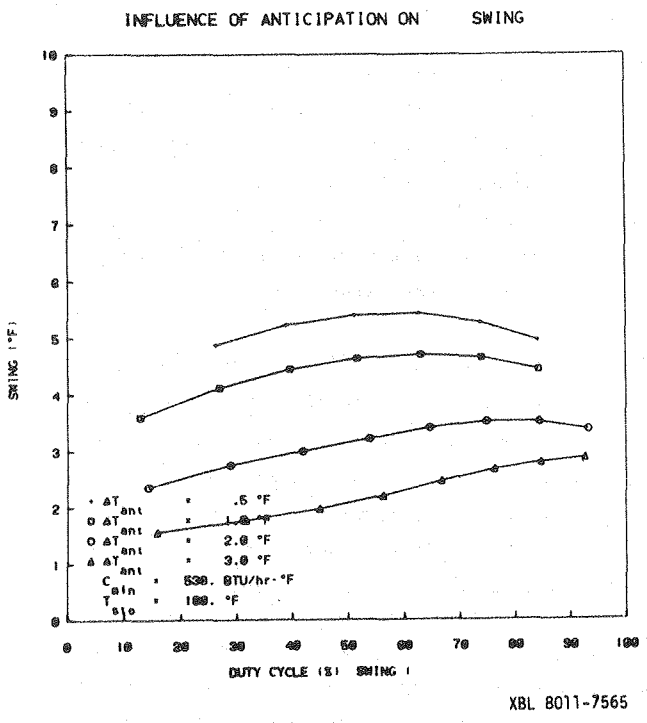

Figure 6. Swing decreases as the anticipation is increased.

ΔT_{ant} °F	T_{sto} °F	P_o kBtu/hr	Rate Cycles/hr	Duty Cycle %	Swing °F	Droop °F
1.0	120	50.	3.0	79.	5.4	-0.6
	140	70.	4.2	61.	7.3	-0.3
	160	90.	4.5	45.	8.5	0.06
	180	110.	4.6	43.	9.8	0.12
2.0	120	50.	4.0	79.	4.3	-1.3
	140	70.	5.6	62.	5.5	-0.9
	160	90.	5.9	52.	6.6	-0.6
	180	110.	6.0	45.	7.5	-0.4
3.0	120	50.	5.2	80.	3.4	-2.1
	140	70.	7.4	64.	4.1	-1.6
	160	90.	7.9	54.	4.8	-1.2
	180	110.	7.9	47.	5.5	-1.0

Table 5. Effect of storage tank temperature and anticipation on cycle rate, duty cycle, swing, and droop for active heating. Outdoor temperature -10 °F. Design heat load 16.8 kW (32 kBtu/hr). C_{min} = 1430 Btu/hr-°F.

Klein, and Duffie [17], the fan coil is sized to give 185 % of the design heat load at a storage tank temperature of 180°F which requires a capacitance rate of C_{min} = 1430 Btu/hr-°F. The cycle performance characteristics for different anticipator gains are summarized in Table 5. For an anticipator gain of 2 °F at an outside temperature of -10 °F, an increase of the storage tank temperature increases the effective heat delivery power and decreases the duty cycle from 79 % at 120 °F to 45 % at 180 °F.

The thermostat reacts more slowly than the room air to heat input. Figure 7 shows the temperature swing as a function of outdoor and storage tank temperature for an anticipator gain of 2 °F. As the effective heat-delivery power is increased, for an outside temperature of -10 °F the room temperature swing also increases from 4.3 °F at a storage temperature of 120 °F to 7.5 °F at 180 °F. The droop decreases from - 1.3 °F at a storage temperature of 120 °F to - 0.4 °F at 180 °F.

As the storage temperature decreases, the droop for a given outside temperature also decreases. However this is only a consequence of the increased duty cycle. When the droop for different storage tank temperatures is plotted as a function of duty cycle for a given anticipator setting, as shown in Figure 8, the result is independent of storage tank temperature.

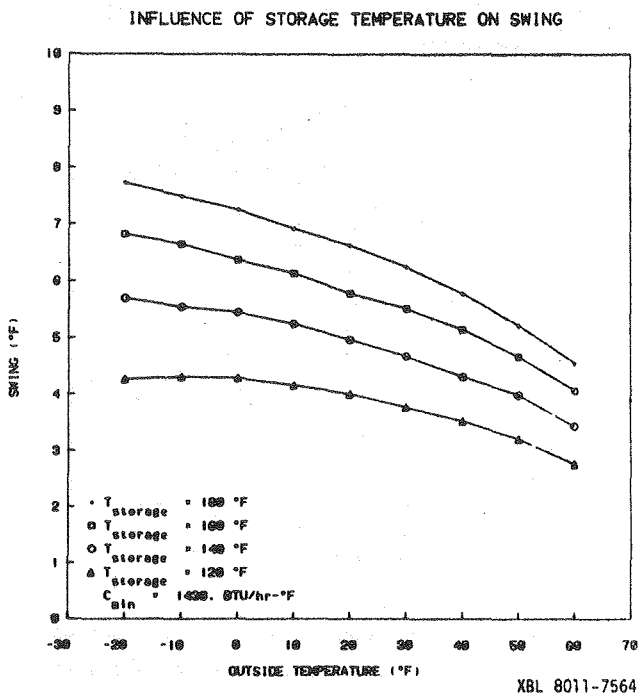

Figure 7. The storage tank temperature influences swing. As the storage tank temperature decreases the swing decreases for a given outdoor temperature.

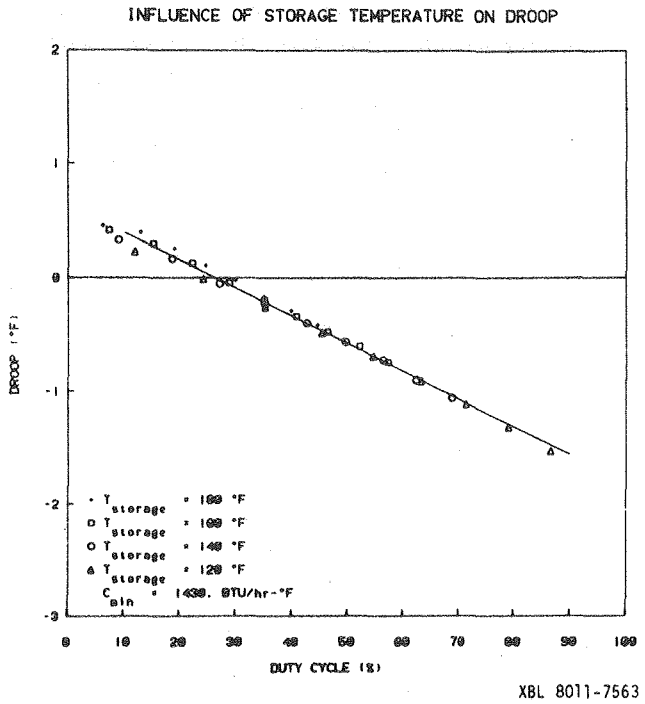

XBL 8011-7563

Figure 8. The droop for a given duty cycle is independent of the storage tank temperature. Thus, the droop is only a function of the anticipation and duty cycle.

CONCLUSIONS

Important variations in the "comfort variables" droop and swing can appear in active solar heating systems with changes in the outdoor and storage tank temperatures. This allows room air temperature to go outside the recommended ASHRAE 55-74R thermal acceptability range at 50 % relative humidity of 20 °C to 23.6 °C (68 °F to 74.5 °F). For given conditions of outdoor temperature, anticipation, and thermostat setpoints, the storage tank temperature (T_{stor}) has a direct effect on duty cycle, droop, and swing. The higher the storage tank temperature, the larger is the swing and the smaller is the droop.

The results confirm that droop, the offset of average room temperature from the thermostat setpoint, is due to the anticipation used in the thermostat that reduces the room air temperature swing. This effect becomes more important with the larger anticipation required to reduce overheating produced by the active solar heating system.

To maintain room temperature within comfort limits, a hydronic solar space heating system will require a control system that adjusts anticipation and setpoints in relation to the outdoor temperature and to the storage tank temperature. This will require a control algorithm more sophisticated than a simple on-off bimetal thermostat. A thermostat can minimize both swing and droop by: adjusting the anticipation depending on outdoor and storage tank temperature to reduce the swing; and compensating for the droop created by the anticipation by adjusting the thermostat setpoints.

Such control can be implemented with analog thermostats using outdoor and storage temperature reset strategies using a three way valve to reduce the fan coil capacity when the storage tank temperature is high and adjusting the thermostat setpoint when the outdoor temperature is low. However, such implementation is awkward and expensive. Effective application of such a control strategy may require the development of thermostats using electronic anticipation to eliminate droop and most likely using a microprocessor to control the heating system.

REFERENCES

[1] M.L. Warren, S.R. Schiller, and M. Wahlig, "Experimental Test Facility for Evaluation of Controls and Control Strategies," Proc. 2nd Systems Simulation and Economic Analysis Conference, San Diego, CA, January 1980. pp. 175-179. Report LBL-10352.

[2] V.R. Anderson & J.R. Tobias, "Comfort control for central electric heating systems", IEEE Transaction on Industry Applications, Vol. IA-10, No. 6, Nov-Dec 1974.

[3] L.W. Nelson, "Predicting control performances of residential heating systems with analog computer", IEEE Transactions on Industry Applications, Vol. IA-10, Nov-Dec 1974.

[4] L.W. Nelson & J.L. Magnussen, "Analytical predictions of residential electric heating system performance", IEEE Transactions on Industry Applications, Vol. IA-10, Nov-Dec 1974.

[5] W.K. Roots, M. Shridar, R.H. Tull, & J.R. Pfafflin, "Mode-dependent time-consultants in three forms of space heating", IEEE Transactions on Industry Applications, Vol. IA-10, No. 6, Nov-Dec 1974.

[6] W.K. Roots, M. Shridar, & R.B Cirjanic, "Improved control strategies for electric space heating processes", IEEE Transactions on Industry Applica-

tions, Vol. IA-10, No. 6, Nov-Dec 1974.

[7] R.O. Zermuehler and H.L. Harrison, "Room Temperature Response to a Sudden Heat Disturbance Input", ASHRAE Transactions, 71, Part I, (1965) pp. 206-210.

[8] H.L. Harrison, W.S. Hansen, and R.E. Zelenski, "Development of a Room Transfer Function Model for Use in the Study of Short-Term Transient Response", ASHRAE Transactions, 74 (1968), pp. 198-206.

[9] K.M. Letherman, "Functional modeling of room temperature responses and the effects of thermostat characteristics on room temperature control", in C.J. Hoogendoorn & N.H. Afgan, Energy Conservation in Heating, Cooling and Ventilating Buildings, (Washington: Hemisphere Publishing Corp., 1978).

[10] M.L. Warren, A.F. Sakkal, and S.R. Schiller, "Predicting the time response of a building under heat input conditions for active solar heating systems,". Proc. 2nd Systems Simulation and Economic Analysis Conference, San Diego, CA, pp.317-322. January 1980. Report LBL-10360.

[11] M.F. McBride, "Measurement of residential thermostat dynamics for predicting transient performance", ASHRAE Transactions, Vol. 85, Part 1. (1979),

[12] M.F. McBride, "Dynamic modeling of system transients by computer simulation for prediction of residential energy consumption", Ph.D. Thesis, Ohio State University, 1979.

[13] W.K. Roots, "Fundamentals of temperature controls", (Academic Press, 1969).

[14] R.H. Socolov & R.C. Sonderegger, "The Twin Rivers Program on Energy Conservation in housing: Four Year Summary Report", Center for Environmental Studies, Report No. 32, August 1976, Princeton University. Excerpts in ASHRAE Transactions, Vol. 83, Part I, (1977).

[15] P.J. Hughes & J.H. Morehouse, "A TRNSYS-compatible, standardized load model for residential system studies", Final report, May 1979, Sciences Applications Inc.

[16] V.C. Miles, "Thermostat control: Principles and practice", (London: Newnes-Butterworths, 1979).

[17] W. A. Beckman, S. A. Klein, and J. A. Duffie, "Solar Heating Design", (New York: John Wiley & Sons, 1977), p.70.